

# A Deep Supervised Lacunarity Analysis Model Based on Weight Adaptive Local Binary Pattern Texture For Palmprint Recognition System

Abirami B<sup>1</sup>, Krishnaveni K<sup>2</sup>

<sup>1</sup>Research Scholar, Research Department of Computer Science, Sri S. Ramasamy Naidu Memorial College, Affiliated with Madurai Kamaraj University, Sattur - 626203, Virudhunagar District, Tamilnadu, India.

<sup>2</sup>Associate Professor, Research Department of Computer Science, Sri S. Ramasamy Naidu Memorial College, Affiliated with Madurai Kamaraj University, Sattur - 626203, Virudhunagar District, Tamilnadu, India.

Email: abirami@vhnsnc.edu.in

DOI: 10.47750/pnr.2023.14.03.258

## Abstract

In this research, a Deep Supervised Lacunarity Analysis Model based on the Weight Adaptive Local Binary Pattern Texture for Palmprint Recognition (DSLPR) system is proposed for evolving the innovative Palmprint Recognition System (PRS). To reveal the originality of DSLPR system, a new Section-based Contour Lacunarity Analysis based on Weight Adaptive Local Binary Pattern (SCLA-WALBP) feature extraction approach and a Deep Learning Network classifier using a Supervised Algorithm (DLNSANet) are implemented to gain the superior substantiation accuracy rate for accessing the digital content and highly worthy assets. To accomplish the DSLPR system, Two Dimensional Palmprint Region of Interest (2D-PROI) image is preprocessed (PI), spotted out all tiny edges, ridges, and wrinkles of PI using Weight Adaptive Local Binary Pattern (WALBP) algorithm, and traced all outlines of the PI using a canny edge detection algorithm. SCLA-WALBP approach is invoked to produce an exclusive feature vector. Classify this feature vector using DLNSANet classifier approach to substantiate the authentic person with more accuracy rate. This research work experiment is employed on PolyU's multi-spectral 2D-PROI image database. This DSLPR system has been appraised with 99% of authentication accuracy.

**Keywords:** Palmprint Recognition System, Deep Learning, Supervised Algorithm, Section-Based Lacunarity Analysis, Local Binary Pattern, Canny Edge Detection Algorithm.

## 1. INTRODUCTION

Several human identification applications are needed for securing the protectiveness in country border, restriction of access, and secure observation in banking, airport and many places [1]. [2] It can be accomplished by authenticating and identifying the humans' asset-based, knowledge-based, and biometrics-based technologies. Nonetheless, humans' asset-based and skill-based technology is uncomplicated to compose, forging and forget [1]. Even so, biometric-based technology is more trustable and securable technology to furnish the high security to the public [1] [3].

Biometric is the technology to recognize the authenticate person using the person's body parts, and conduct-sense traits [2]. Enhancing the efficient of biometric-technology based on the chosen of traits that must offer the high exclusivity, ubiquity, immortality, accumulatively, enactivity, suitability and less eludivity [4]. Amid the face [5][6], fingerprint [7][8], iris [9][10] and gait [11][12] traits, [4] Researchers research the palmprint trait continuously to attain the efficient biometric, because of its rich exclusivity, ubiquity, immortality, and high enactivity [13] [14]. A palmprint image has lots of visible features of a palm such as the line, ridges, and wrinkles [15][16][17]. And that are conserved as the texture feature values used to play a vital role in the authentication processes.

Many local feature extraction approaches, such as fractal-based techniques and Local Binary Pattern (LBP) have been proposed and analysis by Bruno et al., 2008; Mandelbrot, 1983, Ojala et al., 1996, Florindo and Bruno8 (2013); Florindo et al. (2012) [18][3] [19]. Even though, fractal-based and LBP approaches has many inadequacies such as provision of same dimension values to several parts of the image surface (similarity values), noise sensibility, correlated features that are lead the poor classification [18][20][21][22]. Adaptation is needed to all local feature extraction approaches to develop the texture analysis as well as to make the perfect fit for some particular applications [18]. [19] proposed the seven algorithms in presence of rotational changes, noise degradations, contrast information, and various sizes of LBP masks and obtained the poor classification rate upto 80.22%. [18] stated the new texture image descriptor, combining the local binary patterns extracted from the grey-level image (classic approach) and achieved the 93.54% classification rate.

[22] [23] One optimized method to extract the texture features is Model-based texture approach due to its low computation time and processing steps compared to other approaches. [24] [25] Model-based approaches are used to draw out the basic qualitative properties of the texture. [25] In 1970, Mandelbrot introduced a new field of mathematics called fractal to model the coarseness, harshness, and self-similarity in a texture image. [26], [27] Gangepain and Roques-Carnes was invented the Box-Counting algorithm to estimate the fractal dimension values. It has a major problem of offering [Dong/2000, Mandelbrot/1998, vos/1980] same fractal dimension values for distinct texture and appearance of various fractal sets. It could be overcome by the lacunarity approach. [28] [29] [30] [Mandelbrot /1983] introduced the term Lacunarity using Gliding-box algorithm to illustrate the different texture appearances patterns along with same dimension values by specifying different variances or mean values.

After setting the collection of the feature vectors, Machine Learning (ML) and Deep Learning (DL) classifier algorithms are used to perform the authentication and identification processes. [31] ML algorithms are not having the ability to learn the huge datasets because of ambiguity in training and decision making. [32] to overcome the drawbacks of ML algorithms, researchers extend their view of perception into next level that is deep learning algorithms. [33], [34] DL algorithms are having more than one layer for grasping a lot of idiosyncratic features to increase the accuracy of the prediction of correct matching classification. [35] demonstrated that DNN with supervised algorithm (Backpropagation algorithm) reached the higher recognition accuracy of 99.99% compared to other machine learning techniques used in this paper. [35], [36] proofed that the DL has the capability to yield the higher recognition rate for palmprint images.

Accordingly, this proposed novel DSLPR system is accomplished using the SCLA-WALBP feature extraction and DLNSANet classifier approaches. SCLA-WALBP feature extraction is executed using the proposed WALBP and lacunarity approaches to generate a set of feature vector. A suitable DLNSANet classifier algorithm and its configuration are designed for setting the higher rate of recognition and verification precision at a low time. The proposed feature extraction and classification approaches are explained in section 2.

## 2. PROPOSED METHODOLOGY

Deep Supervised Lacunarity Analysis Model based on Weight Adaptive Local Binary Pattern Texture for Palmprint Recognition (DSLPR) system is executed in four levels: 1. Data capturing level, 2. Pre-processing level, 3. Feature extraction level, and 4. Classification or Matching level [1]. The authentication and identification processes of DSLPR are illustrated in Fig.1, and Fig.2.

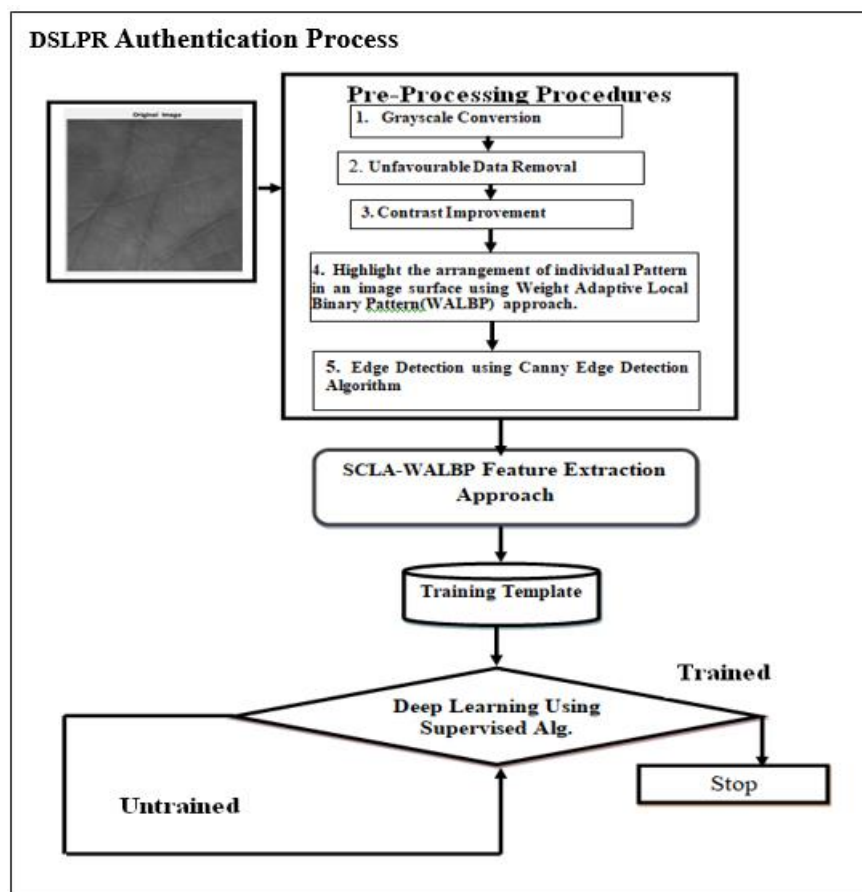


Fig.1. Diagrammatic Representation of DSLPR Authentication Process

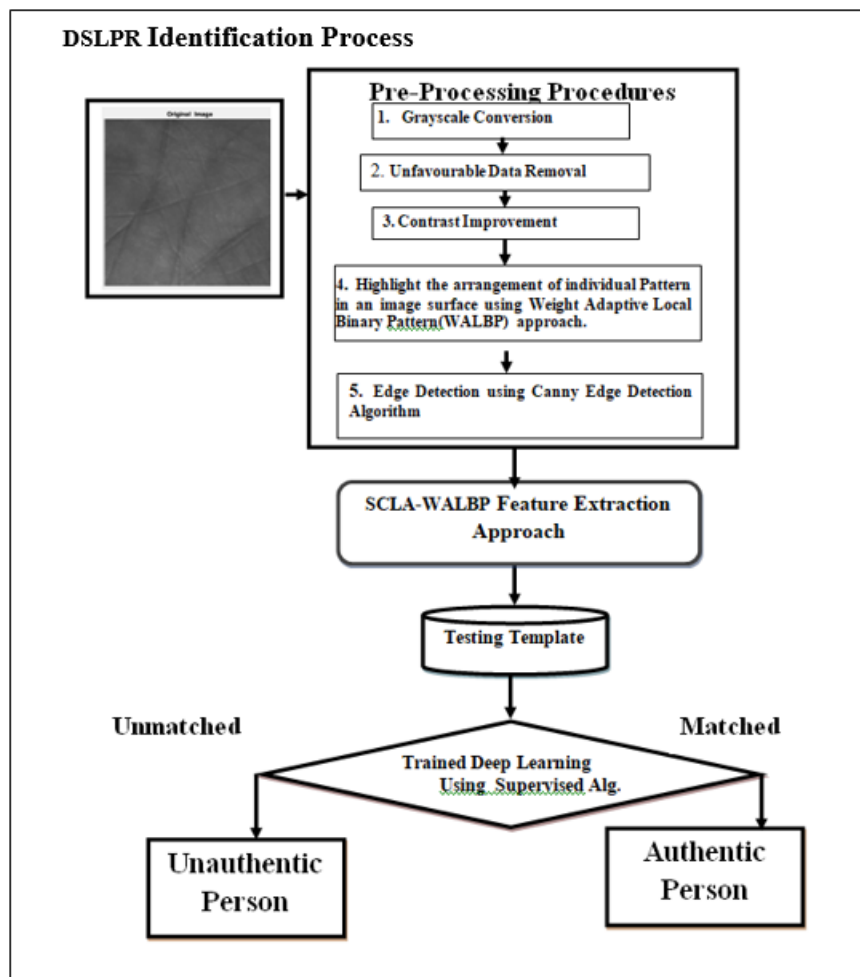


Fig.2. Schematic Diagram of DSLPR Identification Process

### 2.1. Data Acquiring

This research explored the 2D-PROI images of a multi-spectral 2D-ROI palmprint image database at the biometric research center (UGC/CRC) in POLYU, Hong Kong. That is encompassed of 400 volunteers' left and right hands' palms in normalized and segmented .bmp image files, which are put in 10 images of two each discrete section. Few POLYU's biometric research center database 2D-PROI images are shown in Fig. 3.

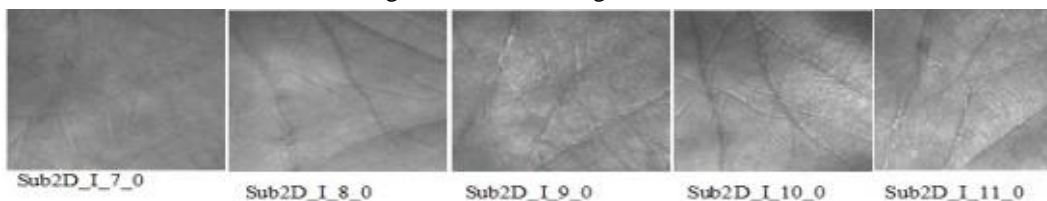


Fig.3. POLYU's Biometric Research Center Database 2D-PROI Images

### 2.2. Pre-processing

The 2D-PROI image is formatted to ameliorate the standard of the image by proceeding the following steps: 1. Gray-scale image conversion, 2. Get rid the irrelevant data in the image, 3. Enlarge the brightness differences in an image to extract the texture information, 4. Highlighting the arrangement of individual pattern in an image surface using WALBP, 5. Outline all creases, lines and ridges of palmprint using Canny edge detection. The Contour pre-processed image is labeled as CPI, and is shown in Fig.4.(a), (b), (c), and (d).

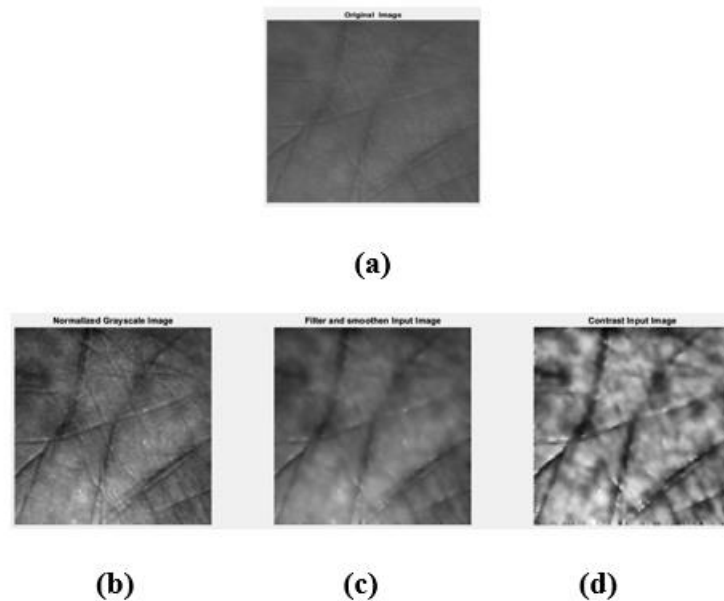


Fig.4. (a) 2DPROI Test Image, (b) Normalized Image, (c) Preprocessed Image, and (d) Contrast Preprocessed Image (PI)

### 2.2.1. Weight Adaptive Local Binary Pattern (WALBP) Algorithm

Weight Adaptive Local Binary Pattern (WALBP) algorithm is a kind of local texture feature extraction approach. It is highlighted the image spatial patterns by determining and replacing the grayscale value differences between centre pixel and neighborhood pixels in the sampling area [26]. It is widely used in image texture feature analysis [46]. The WALBP algorithm is defined in a sampling area (sa) with size of  $3 \times 3$ , and denoted grayscale value of the centre pixel as  $c_0$ , and gray-scale value of 8 pixels around it as  $c_1, c_2, \dots, c_8$ . The sampling code (sc) is generated by comparing each 8-pixel neighbor with the center pixel  $c_0$  as the threshold. When  $c_i \geq c_0$  the corresponding position is encoded with the weighted matrix value  $w_i, i=1,2,3,4,5,6,7,8$  and when  $c_i < c_0$  the corresponding position is encoded with the same centre pixel value  $c_0$ . After all pixels within the sa are coded, the encoding value of 8 pixels around the centre pixel  $c_0$  are highlighted the image texture information, that is shown in Fig.5. Implementation of WALBP can be described as in Fig.6.

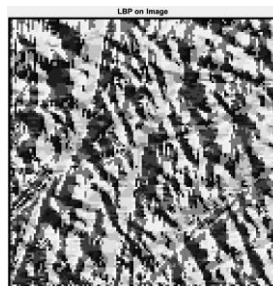


Fig.5. Highlight the Individual Pattern of PI Image using WALBP Algorithm

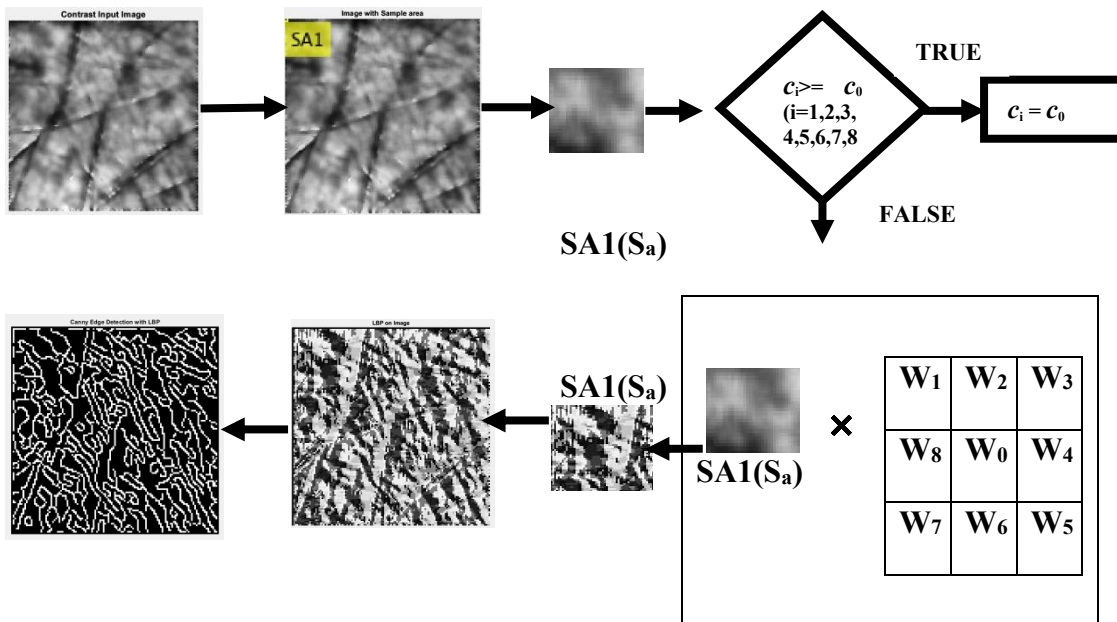


Fig.6. Pictorial Illustration of WALBP Algorithm

After enhancing the spatial patterns of the image, traced the outline edges using a canny edge detection algorithm to extract the more fractal patterns. Fig.7(a) and (b) exhibits the collate of edges on PI image using Canny edge detection algorithm with WALBP and without WALBP algorithm. It divulged more true edges, when applying canny edge algorithm with WALBP algorithm on PI image. Then, PI image is reformed into Contour Pre-processed (CPI) image.

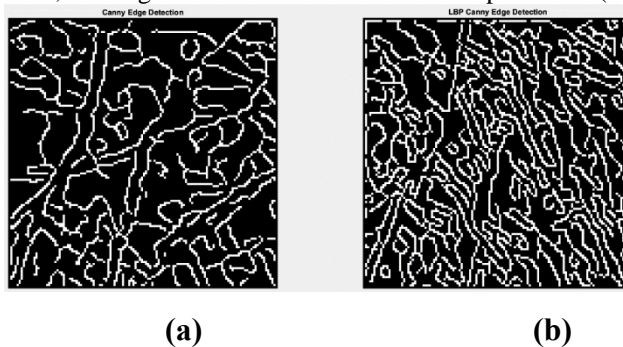


Fig.7. a. CPI Image with Less Edges using Canny Edge Detection Without WLBP Algorithm, b. CPI Image with More Edges using Canny Edge Detection With WLBP Algorithm

In Fig.7 shows the analysis of edges detection on PI image using WLBP algorithm and without using WLBP algorithm. Invoke the canny edge detection using WLBP algorithm reveals more edges that provides more fractal patterns. From the obtained fractal patterns on the CPI image, extract the lacunarity values using Gliding-box approach and stored that as the training and testing template.

### 2.3. Feature Extraction level

A group of isolated Model-based texture features of an image can be efficiently fetched by accomplishing the lacunarity analysis approach. This paper is furnished the Section-based Contour Lacunarity Analysis based on Weight Adaptive Local Binary Pattern (SCLA-WALBP) feature extraction approach to assess the lacunarity values of a CPI image in a distinctive manner and stored it for making the templates. Proposed SCLA-WALBP feature extraction approach is elucidated as below. Fig.9. illustrates the scheme of SCLA-WALBP approach.

#### 2.3.1. SCLA-WALBP approach

The procedure adapted in SCLA-WALBP approach is given below.

Initial step of the executing the SCLA-WALBP approach is to split the CPI image of size  $\Theta \times \Theta$  into four equal sections with the equal size  $\delta \times \delta$  ( $\delta = \Theta / 4$ ) where  $\delta$  refers the each section dimensions.

Each section is declared as (SIs) where s refers to the number of sections i.e. s =1, 2, 3, and 4, which is shown in Fig.8.

Next, the lacunarity values ( $LQ_s$ ) for all section (SIs) are evaluated using Gliding-Box algorithm. The Gliding-Box algorithm was proposed by Allain and Cloitre (1991) [47].

Gliding-Box algorithm begins by sliding the successive coating of an image with the grid of non-overlapping square boxes  $\psi \times \psi$  of set  $\Omega$ , where  $\psi = \delta / \Omega$  at various box scale intervals  $\Omega$ , ( $\Omega = 2, 4, 8, 16, \text{ and } 32$ ). Each square box of set  $\Omega$  contains the collection of pixel intensities  $I(i, j)$  are represented as  $f_{(I_{(i,j)}, \Omega)}$ , where  $i$  and  $j$  represents the index position of the pixel intensity.

And determine the sum of probability of occurrence of all pixel intensities  $P(I(i, j), \Omega)$  within the each square boxes  $\psi \times \psi$  of set  $\Omega$ , using (1).

$$P_{(I_{(i,j)}, \Omega)} = \frac{\sum_{i=1}^{\psi} \sum_{j=1}^{\psi} f_{(I_{(i,j)}, \Omega)}}{N_{\Omega}} \quad | \Omega = 2, 4, 8, 16, \text{ and } 32 |$$

$$| \psi = 1, 2, \dots, \frac{\delta}{\Omega} | \quad | i = 1, 2, \dots, \psi | \quad | j = 1, 2, \dots, \psi | \quad (1)$$

Where  $f_{(I_{(i,j)}, \Omega)}$  refers to the collection of intensity values is placed within the dimension size  $\psi \times \psi$  at various scale interval set  $\Omega$  and  $N_{\Omega}$  refers the number of square boxes in the set  $\Omega$ .

a. Lacunarity ( $L_{\Omega, s}$ ) at various scale  $\Omega$  is measured [47]. Lacunarity value ( $L_{\Omega, s}$ ) for all sections of the CPI image using (2)

$$L_{(\Omega, s)} = \frac{|P_{(I_{(i,j)}, \Omega)}|^{2 \times \sum_{i=1}^{\psi} \sum_{j=1}^{\psi} f_{(I_{(i,j)}, \Omega)}}}{|P_{(I_{(i,j)}, \Omega)}|^{\sum_{i=1}^{\psi} \sum_{j=1}^{\psi} f_{(I_{(i,j)}, \Omega)}^2}}$$

$$| \Omega = 2, 4, 8, 16, \text{ and } 32 | \quad | \psi = 1, 2, \dots, \frac{\delta}{\Omega} | \quad | i = 1, 2, \dots, \psi | \quad | j = 1, 2, \dots, \psi | \quad (2)$$

Where  $P_{(I_{(i,j)}, \Omega)}$  refers the sum of probability of occurrence of all pixel intensities for various scale interval boxes.

b. Finally, the Aggregative lacunarity is determined using (3) to get the unique feature lacunarity values for the entire CPI image.

$$AL_s = \sum_{s=1}^4 L_{(\Omega, s)} \quad | \Omega = 2, 4, 8, 16, \text{ and } 32 | \quad | s=1, 2, 3, \text{ and } 4 | \quad (3)$$



Fig.8. Equal Sector of CPI (labeled as CPI -S1, CPI -2, CPI -S3, and CPI -S4)

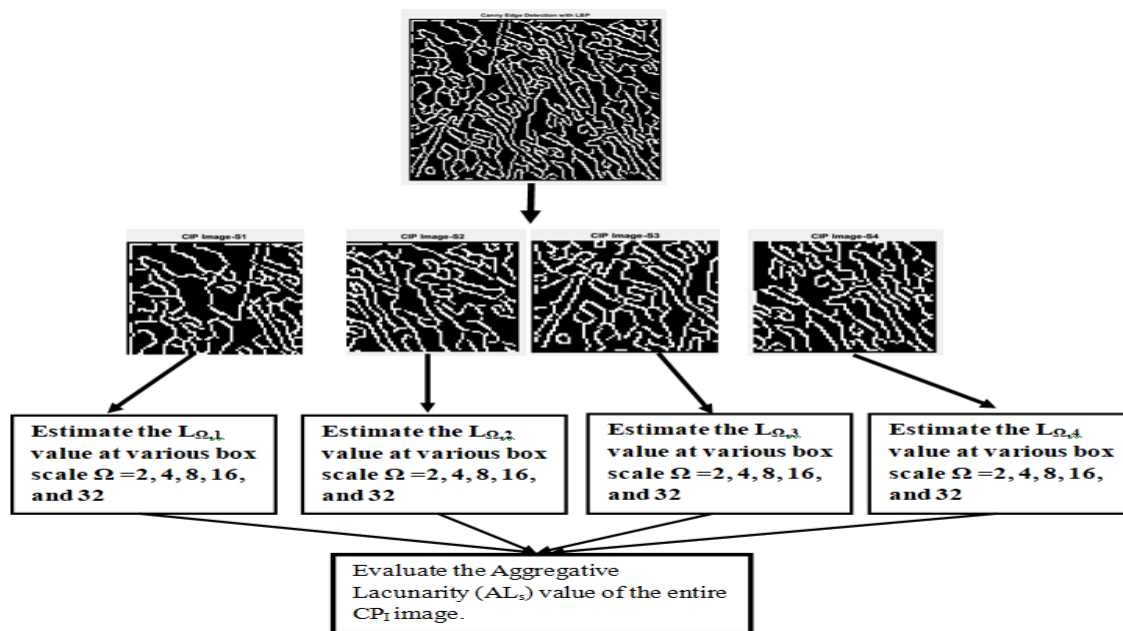


Fig.9. Diagrammatic Illustration of SCLA-WALBP Approach



Thus, the lacunarity values of several 2DPROI images are made out the training and testing template datasets using SCLA-WALBP approach.

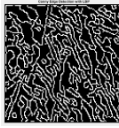


#### 2.4. Classification or Matching level

The Deep Learning Network (DLN) using Supervised Algorithm (DLNSANet) is expanded for constituting the framework. Specification of the DLN is adjusted for grasping the training template exactly in the authentication process. DLN Specifications are delineated in Table.2. Applied the Supervised algorithm (BPANN) on the modulated DLN and used the ReLU and Sigmoid activation functions to obtain the optimized weighted values on all layers. ReLU activation function is computed all layers' output and reinforce it for clearing the complex operations of the determination of previous layers' output [48]. Sigmoid activation function is used to compute the range of 0 to 1 layers' output. At ultimate, all layers in the DLN are observed the optimistic values for authorizing the genuine persons' palmprint. DLNSANet is accessible to learn all various training templates.

### 3. EXPERIMENTAL ANALYSIS

This research is analyzed on 400 left and right-hand 2D-PROI images from the POLYU database. On that, 80% and 20% of 400 images are taken for the palmprint authentication and identification process. In the authentication stage, DLNSANet is trained with various authenticating or training image samples (100, 200, 300 and 400 POLYU's 2D-PROI images). It makes easy learning of all 400 authenticating image samples accurately using DSLPR system. At first, training is deployed on 100 image samples using DLNSANet classifier. [37] Number of training image samples is increased by 100 at each stage to learn the huge datasets gently. At initiate, the specified training and testing image samples are converted into authentication and identification template using the SCALA-LBP feature extraction approach. Those templates are fed into DLNSANet classifier. Table.1 shows the outcome of SCLA-WALBP approach for a test image.

Table 1. Outcome of Lacunarity Values $L_{(\Omega,s)}$ and $AL_s$ using SCLA-WALBP Approach for a Test Image							
Input Image	$\Theta \times \Theta$	$SA_{1..4}$	$\delta \times \delta$	$\Omega$	$\psi \times \psi$	$L_{\Omega}$	$AL_{1..4}$
			32 × 32	2	16 * 16	1.1185	5.1690
				4	8*8	1.0337	
				8	4*4	1.0125	
				16	2*2	1.0037	
				32	1*1	1.0006	
			32 × 32	2	16 * 16	1.1275	5.1709
				4	8*8	1.0308	
				8	4*4	1.0094	
				16	2*2	1.0028	

	128 × 128			32	1*1	1.0004	
			32 × 32	2	16 *16	1.1292	5.1693
				4	8*8	1.0294	
				8	4*4	1.0084	
				16	2*2	1.0020	
				32	1*1	1.0004	
			32 × 32	2	16 *16	1.1296	5.1713
				4	8*8	1.0309	
				8	4*4	1.0079	
				16	2*2	1.0025	
				32	1*1	1.0004	

The DLNSANet classifier has one input, output layer and five hidden layers. The input layer is constituted of four input nodes. ALs values are accommodated on those four input nodes. The output layer is constituted with  $\lfloor \log_2(x) \rfloor + 2$  output nodes where x refers the maximum number of training dataset used in this research work, and five hidden layers are proposed in DLASANet classifier. After the constitution of the DLN, supervised algorithm (BPANN) is implemented on DLN to make the DSLPR system as a learned model. The completion of the DSLPR system learning process is judged by attaining the least Mean Square Error (MSE) values on the training performance graph during the implementation of DLNSANet classifier. Fig.10 is indicated the completion of learning process of DLNSANet classifier by reaching the least MSE at the epoch 7000. The trained DLNSANet classifier is set by the specification is shown in Table.2.

Table 2. Modeled Specifications of DLN-SA Classifier During the Learning Process of DSLPR System

Number of Authenticating Images	Number of Training Factors (Input Nodes)	Number of Output Nodes	Number of Passes	Number of Hidden Layers	Number of Hidden Nodes	Learning Rate
400	4	10	7000	5	36	0.00001

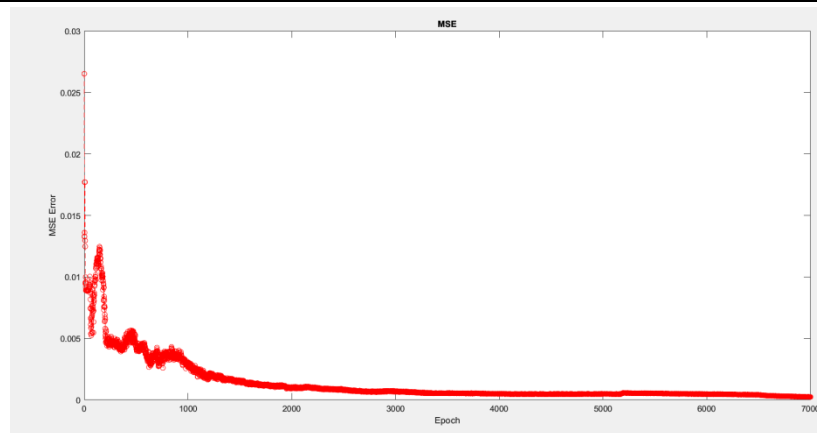


Fig.10. DLNSANet Classifier Performance Graph

Analysis of DSLPR system performance is carried out using confusion matrix's aspects. They are Correct Positive Rate (CPR), True Positive Rate (TPR), False Positive Rate (FPR), Precision, and Specificity. Confusion matrix's aspects can be determined using the value of the diagnostic variables (True Positive (TP), True Negative (TN), False Positive (FP), and False Negative (FN)). Diagnostic variables value can be computed by classifying the accurately matched or not matched the authenticate dataset with the template datasets.

Fig. 11 and Fig. 12 are notified the increasing value of True Positive (TP), TPR (0.9524, 0.9677, 0.1, 0.994) and CPR (0.93, 0.95, 0.9833, 0.99) in every testing dataset. Table.3 implies that the DSLPR system classifies the huge datasets precisely [36]. Table.4 and Fig.13 are exposed the performance of the DSLPR system along with the existing biometric systems' recognition rate. That is proved that the proposed system is one of the optimized systems for accurately identifying the authenticated person.

#### 4. DISCUSSION

This research objective is to contribute the effectual PRS to society by prominence the creation of efficient recognition approaches. Table.3 and Table.4 are revealed the performance of DSLPR system and compared the authentication accuracy

rate of the proposed approaches with other existing recognition approaches to measure the obtained performance scale in its enhancement. Fig. 13 shows the proof of getting 99% authenticating accuracy rate in the DLSPR system which is better than the other authentication approaches used in the accessible biometric technologies. Hence, DLSPR system can be agreed as one of the best authentication systems to secure and control the access of authenticating things and information.

Table 3. Predicted Values and Confusion Matrix Parameters

Number of testing samples	TP	TN	FP	FN	Precision	Specificity	TPR	FPR	CPR
100	80	13	3	4	96.39%	81.25%	95.24%	18.75%	93.00%
200	180	10	4	6	97.83%	71.43%	96.77%	28.57%	95.00%
300	245	50	5	0	98.00%	90.91%	100.00%	9.09%	98.33%
400	330	66	2	2	99.40%	97.06%	99.40%	2.94%	99.00%

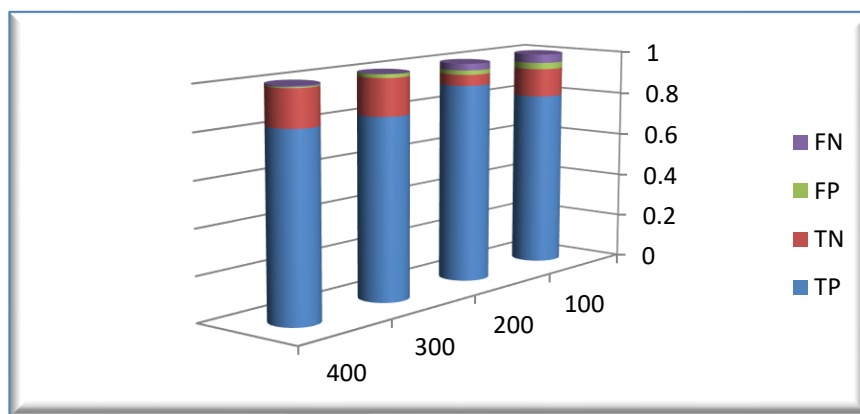


Fig.11. Confusion Matrix's Predicted Values for Various Ranges of Testing Template

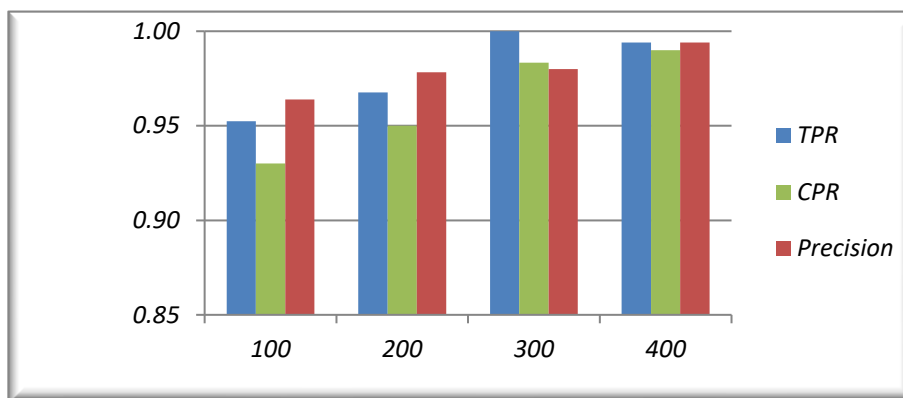


Fig.12. Confusion Matrix Parameter Values for Various Ranges of Testing Template

Table 4. Analysis of Existing Approaches with Proposed Approach

S.No	Recognition Approaches	Recognition Accuracy Rate	Publication year
1.	New Lacunarity Estimation Method + maximum likelihood classifier [37]	81.05%	2000
2.	Differential Lacunarity + DAC, DAC-DF, SVM-RBF, NN Classifiers [38]	94.1%, 94.3%, 94.3%, 94.7%	2012
3.	Lacunarity based DCT + SVM [39]	86.5%	2013
4.	LBP + Lacunarity estimation + SVM-RBF Classifier [40]	98.99%	2014
5.	Fractal Dimension & Lacunarity + ANOVA [41]	78.5%, 94.8%	2015
6.	Fractal Dimension + lacunarity and + multi-fractal dimension + unsupervised classification scheme [42]	72.50%	2017
7.	Histogram+GLCM+GLRLM+lacunarity+MLP Classifier [43]	98.97%	2018
8.	LBP + KNN approaches [44]	90.99%	2020
9.	Fractal dimension, lacunarity, LBP histogram, mean intensity and contrast [45]	90.5%	2021
10.	Generalized dimensions + lacunarity + singularity spectrum + SVM Classifier [46]	98.5%	2021
11.	Proposed approaches (SCLA-WALBP + DLNSANet classifier)	99%	-----

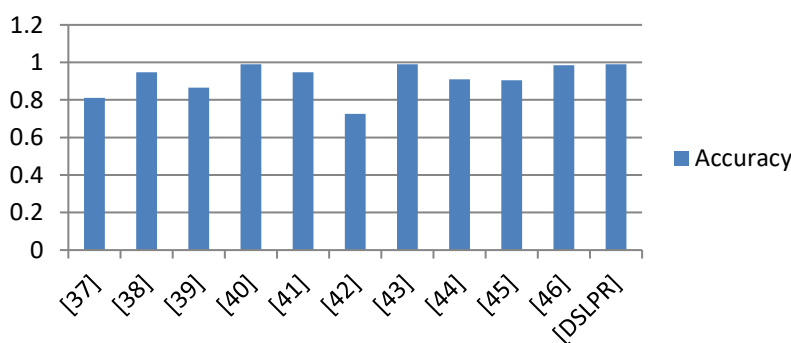


Fig.13. Performance Analysis of Proposed Recognition Approaches with Other Existing Approaches

## 5. CONCLUSION

DLSPR system is developed for making efficient PRS. It is accomplished by innovating a novel feature extraction approach (SCLA-WALBP) to acquire the eccentric texture details of CPI image and that is passed into the DLNSANet classifier to classify the correct authenticated person. This proposed system is tested on 400 POLYU 2D-PROI images and gained a better precision of 99% in the identification process. Wherefore, it will be considered an efficacious BAIS. Nonetheless, the acquirement of indistinguishable texture details in this proposed system met only the 99% accuracy rate in the identification process. It will be overcome in future work by applying the hybrid feature extraction approaches to enhance the methodology to attain a 100% recognition rate in authentication and identification processes.

## REFERENCES

1. Kamboj A, Rani R, Nigam A. A comprehensive survey and deep learning-based approach for human recognition using ear biometric. *Vis Comput.* 2022;38(7):2383-2416. doi: 10.1007/s00371-021-02119-0. Epub 2021 Apr 22. PMID: 33907343; PMCID: PMC8061142. [An Embarking User Friendly Palmprint Biometric Recognition System with Topnotch Security]
2. Goh, Kah Ong Michael & Connie, Tee & Teoh, Andrew. (2008). Touch-Less Palm Print Biometric System.. 2. 423-430.
3. L. Fei, B. Zhang, W. Jia, J. Wen and D. Zhang, "Feature Extraction for 3-D Palmprint Recognition: A Survey," in *IEEE Transactions on Instrumentation and Measurement*, vol. 69, no. 3, pp. 645-656, March 2020, doi: 10.1109/TIM.2020.2964076.

4. X. Wang, X. Tang, "A Unified Framework for Subspace Face Recognition," *IEEE Transactions on Pattern Analysis and Machine Intelligence*, vol. 26, no. 9, pp. 1222–1228, 2004.
5. W. Wang, R. Wang, Z. Huang, S. Shan, X. Chen, "Discriminant Analysis on Riemannian Manifold of Gaussian Distributions for Face Recognition With Image Sets," *IEEE Transactions on Image Processing*, vol. 27, no. 1, pp. 151–163, 2018.
6. X. Si, J. Feng, J. Zhou, Y. Luo, "Detection and Rectification of Distorted Fingerprints," *IEEE Transactions on Pattern Analysis and Machine Intelligence*, vol. 37, no. 3, pp. 555–568, 2015.
7. J. Feng, J. Zhou, A. K. Jain, "Orientation Field Estimation for Latent Fingerprint Enhancement," *IEEE Transactions on Pattern Analysis and Machine Intelligence*, vol. 35, no. 4, pp. 925–940, 2013.
8. M. Zhang, Z. He, H. Zhang, T. Tan, Z. Sun, "Toward practical remote iris recognition: A boosting based framework," *Neurocomputing*, vol. 330, pp. 238–252, 2019.
9. Q. Zhang, H. Li, Z. Sun, T. Tan, "Deep Feature Fusion for Iris and Periocular Biometrics on Mobile Devices," *IEEE Transactions on Information Forensics and Security*, vol. 13, no. 11, pp. 2897–2912, 2018.
10. J. Han, B. Bhanu, "Individual recognition using gait energy image," *IEEE Transactions on Pattern Analysis and Machine Intelligence*, vol. 28, no. 2, pp. 316–322, 2005.
11. C. Wan, L. Wang, V. V. Phoha, "A survey on gait recognition," *ACM Computing Surveys*, vol. 51, no. 5, pp. 1–89, 2018.
12. A. Genovese, V. Piuri, K. N. Plataniotis, F. Scotti, "PalmNet: Gabor-PCA Convolutional Networks for Touchless Palmprint Recognition," *IEEE Transactions on Information Forensics and Security*, pp.1–16, 2019.
13. W. Jia, B. Zhang, J. Lu, Y. Zhu, Y. Zhao, W. Zuo, H. Ling, "Palmprint Recognition Based on Complete Direction Representation," *IEEE Transaction on Image Processing*, vol. 26, no. 9, pp. 4483–4498, 2017.
14. D. Zhang, G. Lu, W. Li, L. Zhang, N. Luo, "Palmprint Recognition Using 3-D Information," *IEEE Transactions on System, Man, and Cybernetics, Part C: Applications and Reviews*, vol. 39, no. 5, pp. 505–519, 2009.
15. X. Wu, D. Zhang, K. Wang, "Palm Line Extraction and Matching for Personal Authentication," *IEEE Transactions on System, Man, and Cybernetics, Part A*, vol. 36, no. 5, pp. 978–987, 2006.
16. F. Yue, B. Li, M. Yu, "Hashing based fast palmprint identification for large-scale databases," *IEEE Transactions on Information Forensics and Security*, vol. 8, no. 5, pp. 769–778, 2013
17. Florindo, João & Bruno, Odemir. (2016). Local fractal dimension and binary patterns in texture recognition. *Pattern Recognition Letters*. 78. 10.1016/j.patrec.2016.03.025.
18. Nava, Rodrigo & Cristobal, Gabriel & Escalante-Ramirez, B. (2012). A comprehensive study of texture analysis based on local binary patterns. *Proceedings of SPIE - The International Society for Optical Engineering*. 8436. 84360E. 10.1117/12.923558.
19. Karperien, Audrey et al. "Reviewing lacunarity analysis and classification of microglia in neuroscience." (2011).
20. Myint, Soe & Lam, Nina. (2005). A Study of Lacunarity-Based Texture Analysis Approaches to Improve Urban Image Classification. *Computers, Environment and Urban Systems*. 29. 501-523. 10.1016/j.compenvurbsys.2005.01.007.
21. He, Xiong & Yang, Zijiang & Zhang, Kun. (2019). Research on Urban Expansion Methods Based on Lacunarity Index. *ICGDA 2019: Proceedings of the 2019 2nd International Conference on Geoinformatics and Data Analysis*. 93-98. 10.1145/3318236.3318237.
22. AnneHumeau-Heurtier, Texture Feature Extraction Methods: A Survey, 2169-3536 2019 IEEE, Volume 7, Digital Object Identifier 10.1109/ACCESS.2018.2890743, (2019).
23. T. Ojala, M. Pietikäinen, and D. Harwood, A comparative study of texture measures with classification based on featured distributions, *Pattern Recognition.*, vol. 29, no. 1, pp. 51–59, (1996).
24. LalehArmi, Shervan Fekri-Ershad, Texture Image Analysis and Texture Image Analysis And Texture Classification Methods – A Review, *International Online Journal of Image Processing and Pattern Recognition Vol. 2, No.1*, pp. 1-29,( 2019).
25. Mrinal Kanti Bhowmik, Anindita Roy, Usha Rani Gogoi, Niharika Naith: Estimation of Architectural Distortion in Mammograms using Fractal features. *IEEE Nuclear Science Symposium and Medical Imaging Conference (NSS/MIC)*, (2017).
26. Gun-Baek So, Hye-Rim So, Gang-Gyoo Jin.: Enhancement of the Box-Counting Algorithm for fractal dimension estimation. *Pattern Recognition Letters*, Volume 98, Pages (53-58) 0167-8655, Elsevier (2017).
27. M. N. Barros Filho, F. J. A. Sobreira, Accuracy of Lacunarity Algorithms in Texture Classification of High Spatial Resolution Images From Urban Areas, *The International Archives of the Photogrammetry, Remote Sensing and Spatial Information Sciences*. Vol. XXXVII. Part B3b. Beijing 2008.
28. S.W. Myint, N. Lam , "A study of Lacunarity based texture analysis approach to improve the urban image classification" Elsevier, *Comput., Environ. and Urban Systems* 29 (2005) 501–523.
29. Xiong He, Zijiang Yang, Kun Zhang, "Research on Urban Expansion Methods Based on Lacunarity Index", *ICGDA*, March 15–17, 2019, Prague, Czech Republic © 2019 Association for Computing Machinery. ACM ISBN 978-1-4503-6245-0/19/03...\$15.00 (2019).
30. Charles R. Tolle\*, Timothy R. Mc Junkin, David J. Gorsich," An efficient implementation of the gliding box lacunarity algorithm" Elsevier – Science Direct - *Physica D* 237 (2008) 306–315,https://doi.org/10.1145/3318236.3318237.
31. Matějka P, Zhang L, Ng T, Mallidi HS, Glembek O, Ma J, et al. Neural Network Bottleneck Features for Language Identification. In: *Proceedings of Odyssey 2014*. vol. 2014. International Speech Communication Association, p. 299–304. Available from: [http://www.fit.vutbr.cz/research/view\\_pub.php?id=10686](http://www.fit.vutbr.cz/research/view_pub.php?id=10686), (2014).
32. Alicia Lozano-Diez, Ruben Zazo, Doroteo T. Toledano, Joaquin Gonzalez-Rodriguez, An analysis of the influence of deep neural network (DNN) topology in bottleneck feature based language recognition, *PLOS ONE* | <https://doi.org/10.1371/journal.pone.0182580>. (August 10, 2017).
33. Djamel Samai1, Khaled Bensid, Abdallah Meraoumia, Abdelmalik Taleb-Ahmed and Mouldi Bedda, 2D and 3D Palmprint Recognition using Deep Learning Method, *IEEE*, 978-1-5386-4238-2/18/\$31.00 © (2008).
34. M.M.Ata, K.M. Elgamily and M.A. Mohamed, "Toward Palmprint Recognition Methodology Based Machine Learning Techniques," *European Journal of Electrical Engineering & Computer Science*, vol. 4, no. 4, 2020.
35. Z. Dandan, P. Xin, L. Xiaoling and G. Xiaojing, "Palmprint Recognition Based on Deep Learning," in *ICWMMN Proceedings*, 2015.
36. T. Kumar, S. Bhushan and S. Jangra, "An Improved Biometric Fusion System of Fingerprint and Face using Whale Optimization", *International Journal of Advanced Computer Science and Applications (IJACSA)*, vol. 12, no. 1, 2021.
37. Dong, P. "Test of a New Lacunarity Estimation Method for Image Texture Analysis." *International Journal of Remote Sensing* 21, no. 17 (2000): 3369–

73. doi:10.1080/014311600750019985.

38. Charisis, Vasileios S., Leontios J. Hadjileontiadis, Christos N. Liatsos, Christos C. Mavrogiannis, and George D. Sergiadis. "Capsule Endoscopy Image Analysis Using Texture Information from Various Colour Models." *Computer Methods and Programs in Biomedicine* 107, no. 1 (2012): 61–74. doi:10.1016/J.CMPB.2011.10.004.
39. A. Eid, V. S. Charisis, L. J. Hadjileontiadis and G. D. Sergiadis, "A curvelet-based lacunarity approach for ulcer detection from Wireless Capsule Endoscopy images," *Proceedings of the 26th IEEE International Symposium on Computer-Based Medical Systems*, 2013, pp. 273-278, doi: 10.1109/CBMS.2013.6627801.
40. Quan, Yuhui & Xu, Yong & Sun, Yuping & Luo, Yu. (2014). Lacunarity Analysis on Image Patterns for Texture Classification. 160-167. 10.1109/CVPR.2014.28.
41. Smitha KA, Gupta AK, Jayasree RS. Fractal analysis: Fractal Dimension and Lacunarity from MR Images for Differentiating the Grades of Glioma. *Phys Med Biol*. 2015 Sep 7;60(17):6937-47. doi: 10.1088/0031-9155/60/17/6937. Epub 2015 Aug 25. PMID: 26305773.
42. Pant, Triloki. (2017). The Role of Fractal Dimension, Lacunarity and Multifractal Dimension for Texture Analysis in SAR Image—A Comparison Based Analysis. 10.1007/978-81-322-3592-7\_13.
43. E. L. Frannita, H. A. Nugroho, A. Nugroho, Zulfanahri and I. Ardiyanto, "Performance of Lacunarity Features for Classifying Thyroid Nodule using Thyroid Ultrasound Images," 2018 2nd International Conference on Imaging, Signal Processing and Communication (ICISPC), 2018, pp. 79-83, doi: 10.1109/ICISPC44900.2018.9006724.
44. F. T. Anggraeny, E. P. Mandyartha and D. S. Y. Kartika, "Texture Feature Local Binary Pattern for Handwritten Character Recognition," 2020 6th Information Technology International Seminar (ITIS), 2020, pp. 125-129, doi: 10.1109/ITIS50118.2020.9320980.
45. A. Concea, T. Nitescu, L. Ichim and D. Popescu, "Texture Analysis for Images with Forested Areas," 2021 23rd International Conference on Control Systems and Computer Science (CSCS), 2021, pp. 197-202, doi: 10.1109/CSCS52396.2021.00039.
46. M. M. Abdelsalam and M. A. Zahran, "A Novel Approach of Diabetic Retinopathy Early Detection Based on Multifractal Geometry Analysis for OCTA Macular Images Using Support Vector Machine," in *IEEE Access*, vol. 9, pp. 22844-22858, 2021, doi: 10.1109/ACCESS.2021.3054743.
47. Filho, Mauro Barros and Fabiano Sobreira. "Accuracy of Lacunarity Algorithms in Texture Classification of High Spatial Resolution Images From Urban Areas" (2008).
48. Y. LeCun, Y. Bengio and G. Hinton, "Deep learning," *Nature*, vol. 521, pp. 436-444, 2015.